Climate Dynamics (2024) 62:1983–1996
https://doi.org/10.1007/s00382-023-07006-z

ORIGINAL ARTICLE

Uncertainty assessment of future climate change using bias-corrected high-resolution multi-regional climate model datasets over East Asia

Changyong Park[1] · Seok-Woo Shin[1] · Ana Juzbašić[1] · Dong-Hyun Cha[1] · Youngeun Choi[2] · Seung-Ki Min[3] · Yeon-Hee Kim[3] · Eun-Chul Chang[4] · Myoung-Seok Suh[4] · Joong-Bae Ahn[5] · Young-Hwa Byun[6]

Received: 8 March 2023 / Accepted: 20 October 2023 / Published online: 20 November 2023

Abstract

The quantitative assessment of the uncertainty components of future climate projections is critical for decision-makers and organizations to establish climate change adaptation and mitigation strategies at regional or local scales. This is the first study in which the changes in the uncertainty components of future temperature and precipitation projections are quantitatively evaluated using multiple regional climate models over East Asia, vulnerable to future climate change. For temperature, internal variability and model uncertainty were the main factors affecting the near-term projections. The scenario uncertainty continued to increase and was estimated to be the dominant factor affecting the uncertainty after the mid-term projections. Although precipitation has the same main uncertainty factors as the temperature in the near-term projections, it considerably differs from temperature because the internal variability notably contributes to the fraction to the total variance, even in the long-term projections. The internal variability of the temperature and precipitation in the near-term projections were predicted to be larger in Korea than that in East Asia. This was confirmed by regional climate models as well as previous studies using global climate models as to the importance of internal variability at smaller regional scales during the near-term projections. This study is meaningful because it provides new possibilities with respect to the consideration of climate uncertainties to the establishment of climate change policies in more detail on the regional scale.

Keywords Uncertainty · Future projection · Climate change · Regional climate model · East Asia

1 Introduction

Climate change is causing notable alterations in the frequency, intensity, spatial extent, duration, and timing of weather and climate extremes. Consequently, unprecedented occurrences of climate extremes have been observed worldwide (IPCC 2012). Therefore, a comprehensive understanding of these extremes at regional spatial scales is essential for effectively coping with natural disasters. Effective climate change mitigation and adaptation strategies require reliable future climate projections. However, despite considerable advancements in climate modeling, a large range of plausible future climate projections remains as "the uncertainty range" (IPCC 2013), reducing confidence in future projections (Hawkins and Sutton 2009, 2011) making decision-making difficult.

To obtain more reliable information on future climate projections, uncertainty components and their effects should be quantitatively assessed. This is because it is important for decision-makers and organizations to establish climate

✉ Dong-Hyun Cha
dhcha@unist.ac.kr

[1] Department of Urban and Environmental Engineering, Ulsan National Institute of Science and Technology, Ulsan, Republic of Korea

[2] Department of Geography, Konkuk University, Seoul, Republic of Korea

[3] Division of Environmental Science and Engineering, Pohang University of Science and Technology, Pohang, Republic of Korea

[4] Department of Atmospheric Science, Kongju National University, Kongju, Republic of Korea

[5] Department of Atmospheric Science, Pusan National University, Busan, Republic of Korea

[6] National Institute of Meteorological Sciences, Seogwipo, Republic of Korea

change adaptation and mitigation strategies, especially at regional or local scales. Furthermore, future climate uncertainty has important implications for climate change adaptation in various application sectors. This is because a more considerable uncertainty will lead to higher costs and challenges related to the management of climate change adaptation (Giorgi 2010). In other words, reducing the uncertainty according to the future climate could potentially bring enormous economic value. Therefore, if national and local governments establish adaptation policies for various fields vulnerable to future climate change by understanding the uncertainties of future climate projections, it will help reduce unnecessary costs and prevent disasters (Hawkins and Sutton 2009). Because of its large population and extensive industrialized areas, East Asia is vulnerable to future increases in weather and climate extremes as well as sea-level rise due to global warming (IPCC 2012). Therefore, the importance of climate change adaptation and mitigation is emphasized in this region, which requires a better understanding of the uncertainty of future climate projections.

Many studies assessing uncertainties of future climate change have been carried on at the global scale or European region (Knutti et al. 2008; Hawkins and Sutton 2009, 2011; Yip et al. 2011; Booth et al. 2013; Northrop and Chandler 2014; van Pelt et al. 2014; Chen and Sun 2015; Hawkins et al. 2016; Woldemeskel et al. 2016; Evin et al. 2019, 2021; Fernández et al. 2019; von Trentini et al. 2019; Lehner et al. 2020; Zhou et al. 2020). However, very few comprehensive studies have been conducted regarding the uncertainty of climatic projections over East Asia. Furthermore, in most previous studies, global climate models (GCMs) were applied, which are limited to the detailed assessment of the uncertainty of future climate change at the regional scale.

To resolve insufficient GCM simulations with a coarse spatial resolution at the regional scale, the Coordinated Regional Climate Downscaling Experiment (CORDEX) project, covering 14 regional domains, has been established by the World Climate Research Programme (WCRP). This project produces diverse regional climate models (RCMs) to provide quality-controlled information about regional climate changes (Giorgi et al. 2009; Park et al. 2021; http://wcrp-cordex.ipsl.jussieu.fr/). For the East Asia domain, RCMs with various spatial resolutions forced by various GCMs produced by the CORDEX East-Asia project team have been applied to several future climate information studies for East Asia (Kim et al. 2014; Park et al. 2016, 2020a, 2021; Lee et al. 2019; Park and Min 2019; Kim et al. 2020a, b) and the Korean Peninsula regions (Ahn et al. 2015; Cha et al. 2016; Choi et al. 2016; Oh et al. 2016; Suh et al. 2016; Lee et al. 2017; Kim et al. 2018). In phase II of the CORDEX-East Asia project, climate change scenarios for RCMs forced by various GCMs have been produced, which exhibited a higher spatial resolution (25-km) than those of phase I (50-km). Therefore, to obtain detailed and reliable future climate change information for the East Asia domain, the quantitative assessment of the uncertainty components for future climate projections from various RCMs produced by the CORDEX-East Asia project team is necessary.

This is the first study in which the changes in the uncertainty components of future temperature and precipitation projections were quantitatively evaluated on the regional scale in East Asia by using high-resolution multi-RCM datasets. In other words, this study is meaningful in that it provides a new possibility for considering climate uncertainties to the establishment of climate change policies in more detail on the regional scale, in contrast to spatially limited studies of the uncertainty of future projections using GCMs. The remainder of this paper is structured as follows. The observational data, model simulations, and main analysis methods are introduced in Sect. 2. The fractional uncertainties and the fraction of each component to the total variance for the future temperature and precipitation projections over East Asia for the bias-corrected RCM datasets are assessed in Sect. 3. Finally, conclusions and discussions are presented in Sect. 4.

2 Data and methods

2.1 Observational data and model simulations

We selected the land area over East Asia (100° E–150° E and 20° N–50° N) as the analysis domain, which includes Korea, Japan, China (except for the western arid region), and parts of Mongolia and Russia. The major analysis variables are the daily mean surface temperature (TAS) and daily precipitation (PR). The TAS and PR were evaluated as annual mean of the daily value. Moreover, they were assessed in the boreal summer (June–July–August) and boreal winter (December–January–February), which are the characteristic seasons in East Asia. The Asian Precipitation-Highly Resolved Observational Data Integration Toward Evaluation (APHRODITE) reanalysis dataset was used as the reference data for the RCM bias correction (Yatagai et al. 2012), which will be presented in Sect. 2.2. Multiple RCM datasets forced by three Climate Model Intercomparison Project phase 5 (CMIP5) GCMs [HadGEM2-AO (Hadley Centre Global Environmental Model version 2 Atmosphere and Ocean), MPI-ESM-LR (Max Planck Institute Earth System Model Low-Resolution), and GFDL-ESM-2M (GFDL Earth System Model 2M)] included in the CORDEX-East Asia phase II project were used to estimate the uncertainties of future climate projections in this study. The selected three GCMs show more accurate simulations of the East Asian climate compared to other CMIP5 GCMs (Martin et al. 2011; Baek et al. 2013; Sperber et al. 2013; Yoon et al. 2015; Guo et al.

2016). In this study, a total of nine RCMs from five different types were applied. The configurations of nine RCMs are presented in Table 1. The HadGEM3-RA (Hadley Centre Global Environmental Model version 3 Regional Climate Model) and CCLM (COSMO-CLM) were forced by the HadGEM2-AO and MPI-ESM-LR GCMs. The SNURCM (Seoul National University Regional Climate Model) was forced by the MPI-ESM-LR GCM, while WRF (Weather Research and Forecasting model) was forced by the MPI-ESM-LR and GFDL-ESM-2 M GCMs. Lastly, RegCM4 (Regional Climate Model 4) was forced by the HadGEM2-AO and GFDL-ESM-2 M GCMs. The horizontal spatial resolution of all nine RCMs applied in this study is 25 km. Four non-hydrostatic (HadGEM3-RA, CCLM, SNURCM, and WRF) and one hydrostatic (RegCM4) RCM types were used as dynamic frameworks for climate experiments over East Asia. The historical experiment for 1981–2005 and Representative Concentration Pathway (RCP) 2.6 and RCP 8.5 scenarios for 2006–2099 were applied in this study. The RCP2.6 and RCP8.5 scenarios are bipolar in the RCP greenhouse gas emission scenarios. Amongst the RCP scenarios, the RCP2.6 scenario is the closest to the response of the Paris Agreement, and the RCP8.5, 'the worst scenario' determined by IPCC (2013) and Hausfather and Peters (2020), is a scenario based on which the greenhouse gas emissions are maintained at the present level.

2.2 Analysis methods

2.2.1 Bias correction

The RCM datasets suitable for simulating the magnitude of climate change at the regional scale have systematic biases. Because these biases reduce the reliability of future climate projections, it is desirable to apply the bias correction technique to the RCM to remove problems that may arise from future climate simulations (Giorgi and Mearns 1999; Teutschbein and Seibert 2012; Kim et al. 2020a, b; Park et al. 2021). Therefore, the bias correction technique was applied to all RCMs used in this study to assess the uncertainty of future climate change in East Asia. The variance scaling (VS) and quantile mapping of the entire period (QME) were applied to the TAS and PR for each grid, respectively. Then, we applied this to the East Asian average for analysis.

The VS method is suitable for the stepwise correction of both the mean and variance of TAS time series (Teutschbein and Seibert 2012; Kim et al. 2020b). In the first step, the TAS is updated with the help of an additive term based on the difference between the long-duration monthly mean APHRODITE reanalysis dataset and historical experiment datasets. The additive terms are assumed to remain unvaried, even under future conditions.

$$TAS^{*1}_{Hist}(\mathrm{d}) = TAS_{Hist}(d) + \mu_m\left(TAS_{obs}(d)\right) - \mu_m\left(TAS_{Hist}(d)\right) \quad (1)$$

$$TAS^{*1}_{RCP}(\mathrm{d}) = T_{RCP}(d) + \mu_m\left(T_{obs}(d)\right) - \mu_m\left(T_{Hist}(d)\right), \quad (2)$$

where μ_m and (d) are the monthly mean and daily values, respectively; the sub- or superscripts *1, *2, or *3 indicate the bias-corrected dataset of an intermediate step; and * represents the final bias-corrected result. Subsequently, the mean-corrected TAS of the historical experiment $TAS^{*1}_{Hist}(\mathrm{d})$ and that of the RCP scenarios $TAS^{*1}_{RCP}(\mathrm{d})$ are shifted to a zero mean every month:

$$TAS^{*2}_{Hist}(\mathrm{d}) = TAS^{*1}_{Hist}(\mathrm{d}) - \mu_m\left(TAS^{*1}_{Hist}(\mathrm{d})\right) \quad (3)$$

$$TAS^{*2}_{RCP}(\mathrm{d}) = TAS^{*1}_{RCP}(\mathrm{d}) - \mu_m\left(TAS^{*1}_{RCP}(\mathrm{d})\right) \quad (4)$$

The standard deviations [σ of the shifted data $TAS^{*2}_{Hist}(\mathrm{d})$ and $TAS^{*2}_{RCP}(\mathrm{d})$] were then corrected based on the ratio of the observed σ value and σ of the historical experiment.

Table 1 Configurations of the RCMs used in this study

	HadGEM3-RA	CCLM	SNURCM	WRF	RegCM4
GCMs	HadGEM2-AO and MPI-ESM-LR	HadGEM2-AO and MPI-ESM-LR	MPI-ESM-LR	MPI-ESM-LR and GFDL-ESM-2 M	HadGEM2-AO and GFDL-ESM-2 M
Number of grid points, latitude × longitude)	251 × 396	251 × 396	260 × 405	250 × 395	249 × 394
Vertical levels	63 eta	Hybrid-40	24 sigma	30 eta	23 sigma
Dynamic framework	Non-hydrostatic	Non-Hydrostatic	Non-hydrostatic	Non-hydrostatic	Hydrostatic
Convection scheme	Revised mass flux	Tiedtke	Kain-Fritch II	Betts and Miller	MIT-Emanuel
Land surface model	Joint UK Land Environment Simulator (JULES)	TERRA ML	NCAR CLM3	Noah	NCAR CLM3.5
Reference	Davies et al. (2005)	Rockel et al. (2008)	Cha and Lee (2009)	Skamarock et al. (2005)	Giorgi et al. (2012)

$$TAS^{*3}_{Hist}(\mathrm{d}) = TAS^{*2}_{Hist}(\mathrm{d}) \times \left[\frac{\sigma_m(TAS_{obs}(d))}{\sigma_m(TAS^{*2}_{Hist}(\mathrm{d}))}\right] \quad (5)$$

$$TAS^{*3}_{RCP}(\mathrm{d}) = TAS^{*2}_{RCP}(\mathrm{d}) \times \left[\frac{\sigma_m(TAS_{obs}(d))}{\sigma_m(TAS^{*2}_{RCP}(\mathrm{d}))}\right] \quad (6)$$

Finally, the σ-corrected TAS is shifted back using the corrected mean TAS and Eqs. (7) and (8).

$$TAS^{*}_{Hist}(\mathrm{d}) = TAS^{*3}_{Hist}(\mathrm{d}) + \mu_m\left(TAS^{*1}_{Hist}(\mathrm{d})\right) \quad (7)$$

$$TAS^{*}_{RCP}(\mathrm{d}) = TAS^{*3}_{RCP}(\mathrm{d}) + \mu_m\left(TAS^{*1}_{RCP}(\mathrm{d})\right) \quad (8)$$

The QME method is suitable for the precipitation. We performed pre-processing corrections for days with 0 mm precipitation by comparing the empirical cumulative distribution function (ECDF) of observations and models before applying the QME method to the cumulative distribution function (CDF) for bias correction (Kim et al. 2020b). The CDF is based on the generalized extreme value (GEV) distribution and the variable x is as follows:

$$F(x;\mu,\sigma,\xi) = \begin{cases} exp\left[-exp\left\{-\frac{x-\mu}{\sigma}\right\}\right], \xi = 0 \\ exp\left[-\left\{1+\xi\frac{x-\mu}{\sigma}\right\}^{-\xi^{-1}}\right], \xi \neq 0, 1+\xi\frac{x-\mu}{\sigma} > 0 \end{cases} \quad (9)$$

where μ, σ, and ξ are the location, scale, and shape parameters, respectively, which are estimated from the L-moments. The CDF of each RCM, estimated using daily precipitation values from the historical experiment, is fitted to that of the observation dataset (Eqs. (2) and (3)).

$$P^{*}_{Hist}(\mathrm{d}) = F^{-1}_{obs}\left(F_{Hist}\left(P^{*1}_{Hist}(d)|\mu_{Hist},\sigma_{Hist},\xi_{Hist}\right)|\mu_{obs},\sigma_{obs},\xi_{obs}\right) \quad (10)$$

$$P^{*}_{RCP}(\mathrm{d}) = F^{-1}_{obs}\left(F_{Hist}\left(P^{*1}_{RCP}(d)|\mu_{Hist},\sigma_{Hist},\xi_{Hist}\right)|\mu_{obs},\sigma_{obs},\xi_{obs}\right), \quad (11)$$

where P and F are the precipitation and CDF, respectively.

2.2.2 Uncertainty decomposition of future climate projection

We assessed the spatiotemporal changes in the fractions of three uncertainty components to the total variance calculated based on the 1981–2005 mean over East Asia using the method suggested by Hawkins and Sutton (2009, 2011). Based on this method, the rates of change of three spatiotemporal uncertainty components are quantitatively determined (Hawkins and Sutton 2009, 2011; IPCC 2013; Lopez-Cantu et al. 2019; Zhou et al. 2020): internal variability, model uncertainty, and scenario uncertainty. The internal variability, which arises in the absence of any radiative forcing from the planet, consists of the natural variability of the climate system (e.g., the variability of the El Niño–Southern Oscillation, ENSO). Each model projection is fitted to a fourth-order polynomial using the least squares from 1981 to 2099. The raw projection is as follows:

$$X_{m,s,t} = x_{m,s,t} + i_{m,s} + \varepsilon_{m,s,t}, \quad (12)$$

where the reference value is indicated by i, the fit is represented by x, and the residual is ε. The reference values applied were the year 2000. Moreover, the subscripts m, s, and t refer to the model, scenario, and year, respectively. Based on Eq. (12), the internal variability (IV) is calculated as the variance of the residuals of the fits, which is independent of the scenario and year. The multi-model mean of these variances is considered the internal variability component,

$$IV = \frac{1}{N_m}\sum_{m} var_{s,t}(\varepsilon_{m,s,t}), \quad (13)$$

where N_m denotes the number of models and $var_{s,t}$ is the variance of the scenarios and year. The parameter IV remains constant over time. The model uncertainty (MU) of each scenario is estimated from the variance of the different model projection fits. The model uncertainty is the response to structural differences due to the scheme and parameters applied to the models the same radiative forcing, which leads to differences in the simulated climate systems among different models under the fixed RCP scenario. The multi-scenario mean is applied as an estimate of the model uncertainty component,

$$MU(t) = \frac{1}{N_s}\sum_{s} var_m(x_{m,s,t}), \quad (14)$$

where N_s indicates the number of RCP scenarios. The scenario uncertainty (SU), which is related to the anthropogenic forcing, can be defined as the spread of projections between different RCP scenarios, estimated the variance of the multi-model mean for scenarios.

$$SU(t) = var_s\left(\frac{1}{N_m}\sum_{m} x_{m,s,t}\right) \quad (15)$$

Based on the assumption that the three uncertainty components are independent, the total variance (T) of the future climate change projections and the mean change of all projections (G) can be expressed as:

$$T(t) = IV + MU(t) + SU(t) \quad (16)$$

$$G(t) = \frac{1}{N_s}\sum_{m,s} x_{m,s,t}. \quad (17)$$

The fraction of each component to the total variance for the future projection, as presented (c) and (d) in Figs. 3, 4, 5 and 6, is calculated as the respective fractions of IV, $MU(t)$, and $SU(t)$ with respect to $T(t)$ in Eq. (16) (e.g., *The fraction of* $IV = \left(\frac{IV}{T(t)}\right) \times 100$).

The total fractional uncertainty ($FU(t)$) for the future projection with a 90% confidence level can be written as:

$$FU(t) = \frac{1.65\sqrt{T(t)}}{G(t)}. \tag{18}$$

The fractional uncertainty of each component for the future projection as presented (a) and (b) in Figs. 3, 4, 5 and 6, is computed by substituting $T(t)$ with IV, $MU(t)$, and $SU(t)$, respectively, in Eq. (18).

The signal-to-noise (S/N) ratio is obtained by inverting the fractional uncertainty. If the S/N ratio exceeds 1, it indicates that the prediction has excellent value for planning purposes (Hawkins and Sutton 2009, 2011). A maximum S/N ratio corresponds to a minimum total fractional uncertainty (Hawkins and Sutton 2009).

3 Results

The temporal changes in the 10-year moving average of area-averaged future projections, which are calculated based on 1981–2005 mean for the bias-corrected annual and seasonal means from TAS and PR over East Asia, are presented in Fig. 1. The thin solid lines indicate each RCM time series, and the thick solid lines represent the multi-model ensemble (MME) time series of each RCP scenario used in this study. In the case of TAS, the RCP2.6 scenario is expected to remain stable for the annual and all-seasonal means, without large increases and decreases until the end of the twenty-first century. In contrast, the RCP8.5 scenario exhibits continuously rising trends. By the end of the twenty-first century, the annual and all-seasonal means of TAS are expected to increase by up to 3 ℃. The spreads between RCMs in winter are larger than in summer or on the annual scale. Based on the graphs, it can be inferred that the scenario uncertainty will increase after the middle of the twenty-first century. For the PR, the variability of time series in each RCM and the spreads between RCMs are large with respect to the annual and all-seasonal means. The difference between the scenarios is very small, except for winter. Therefore, it can be estimated that the scenario uncertainty is small, except for winter. In the RCP8.5 scenario, the area-averaged winter MME time series over East Asia is expected to decrease slightly by the mid-twenty-first century and then increase by the end of the twenty-first century. This result was led by two HadGEM3-RA RCMs with large projections at the end of the twenty-first century, forced by HadGEM2-AO and MPI-ESM-LR GCMs.

We used cascade plots to express area-averaged future climate projections and uncertainties between models or scenarios for the future three periods of decadal means (2020s, 2050s, and 2090s) over East Asia (Fig. 2). The uncertainty cascade plot is an intuitive tool that can be used to identify the contribution of uncertainty components (e.g., model spreads and scenario ranges) to total variances. The lowest points represent model spreads as the future projections of RCMs. The middle points are the MME values averaging RCMs for the same scenario, and scenario ranges can be

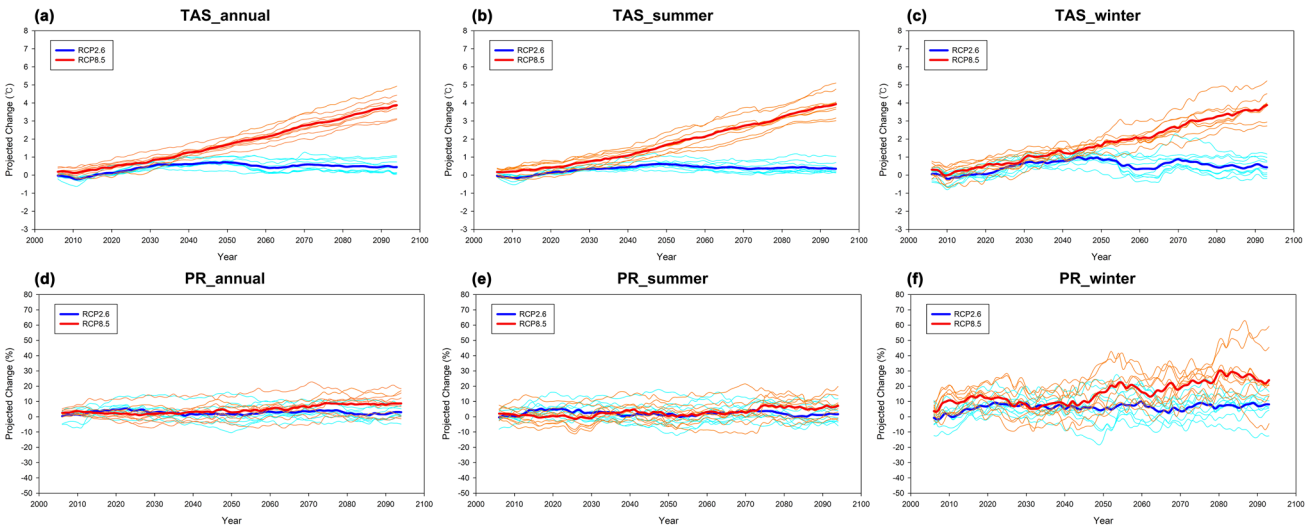

Fig. 1 Temporal changes in the 10-year moving average for area-averaged future projections calculated based on the 1981–2005 mean for the bias-corrected annual and seasonal means of TAS and PR over East Asia. The thin solid lines indicate each RCP model time series and the thick solid lines represent the MME time series for each RCP scenario

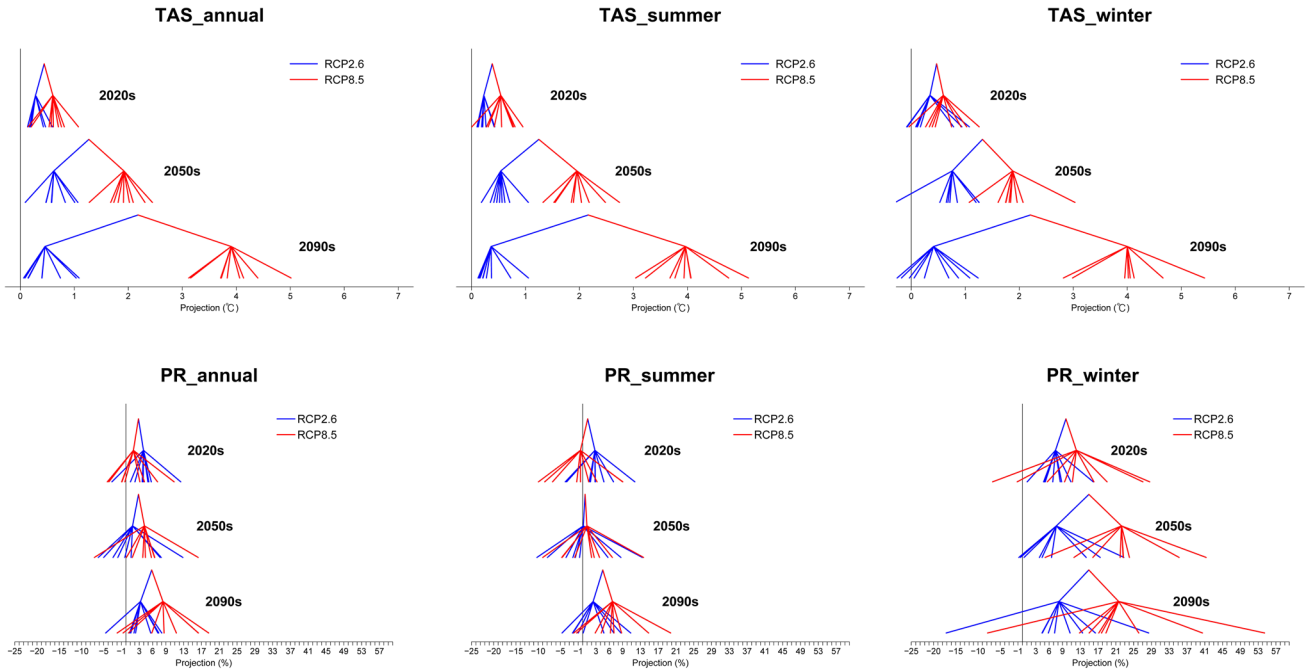

Fig. 2 Cascade plots of future projections calculated based on 1981–2005 mean for the bias-corrected annual and seasonal means of TAS and PR for the future three periods of decadal means over East Asia

identified through them. The top point is the average of the MME for each scenario. Most RCMs, except for a few RCMs in the winter RCP2.6 scenario, yield positive projections for the annual and all-seasonal means of TAS. The model spreads inconsiderably differ depending on the period in the RCP2.6 scenario, while those of the RCP8.5 scenario are predicted to widen over time. In the MME projection for each scenario, the RCP8.5 scenario projects increase over time. However, the RCP2.6 scenario yields a slight increase in the 2050s and, in the 2090s, the positive projection decreases to the level of the 2020s. Consequently, the difference between the MME projections of the two scenarios increases with time. In contrast to the TAS, the annual and all-seasonal means of PR show that the model projections in each scenario are inconsistent in all periods. The MMEs for the two scenarios in the annual and winter means have positive projections, and the overall scenario ranges and model spreads are predicted to widen with time.

We examined the fractional uncertainties and the fraction of each component to the total variance for the future TAS and PR projections for the bias-corrected RCMs over East Asia (Figs. 3, 4, 5 and 6). For the annual and all-seasonal means of TAS from the near-term projection up to approximately the 2020s, most of the uncertainties have resulted from the internal variability and model uncertainty. In contrast, the scenario uncertainty has a minimal contribution. The internal variability and model uncertainty rapidly decrease until the 2040s as the warming intensifies and then gradually decrease (Fig. 3a). Furthermore, by the 2040s, the internal variability declines more than the model uncertainty. Due to the changes in these two uncertainty components, the total fractional uncertainty is smallest in approximately the 2040s; after this period, the scenario uncertainty increases rapidly (Fig. 3c). Interestingly, these results of applying RCMs to the regional scale are consistent with those of previous studies conducted on the global scale using GCMs (Stott and Kettleborough 2002; Cox and Stephenson 2007; Hawkins and Sutton 2009; 2011). The 2030s to 2050s is the reference period to which most long-term climate change adaptation policies until the 2090s are applied. The smallest total fractional uncertainty in this period has an important meaning (Cox and Stephenson 2007). The internal variability is the uncertainty caused by the natural variability that occurs independently of the radiative forcing and increases at smaller spatial or shorter time scales (Hawkins and Sutton 2009). Based on the near-term projection, South Korea's internal variability with respect to the fractional uncertainty and the fraction to the total variance will be larger than that of East Asia (Fig. 3b, d). These findings confirm the importance of the internal variability in decision-making for effective climate change adaptation in the near-term future at smaller regional scales, even in the RCM. In the case of the seasonal TAS uncertainty over East Asia, it is expected that summer will have the fractional uncertainty and the fraction to the total variance, which are almost similar to the annual mean results (Fig. 4a–d). On the

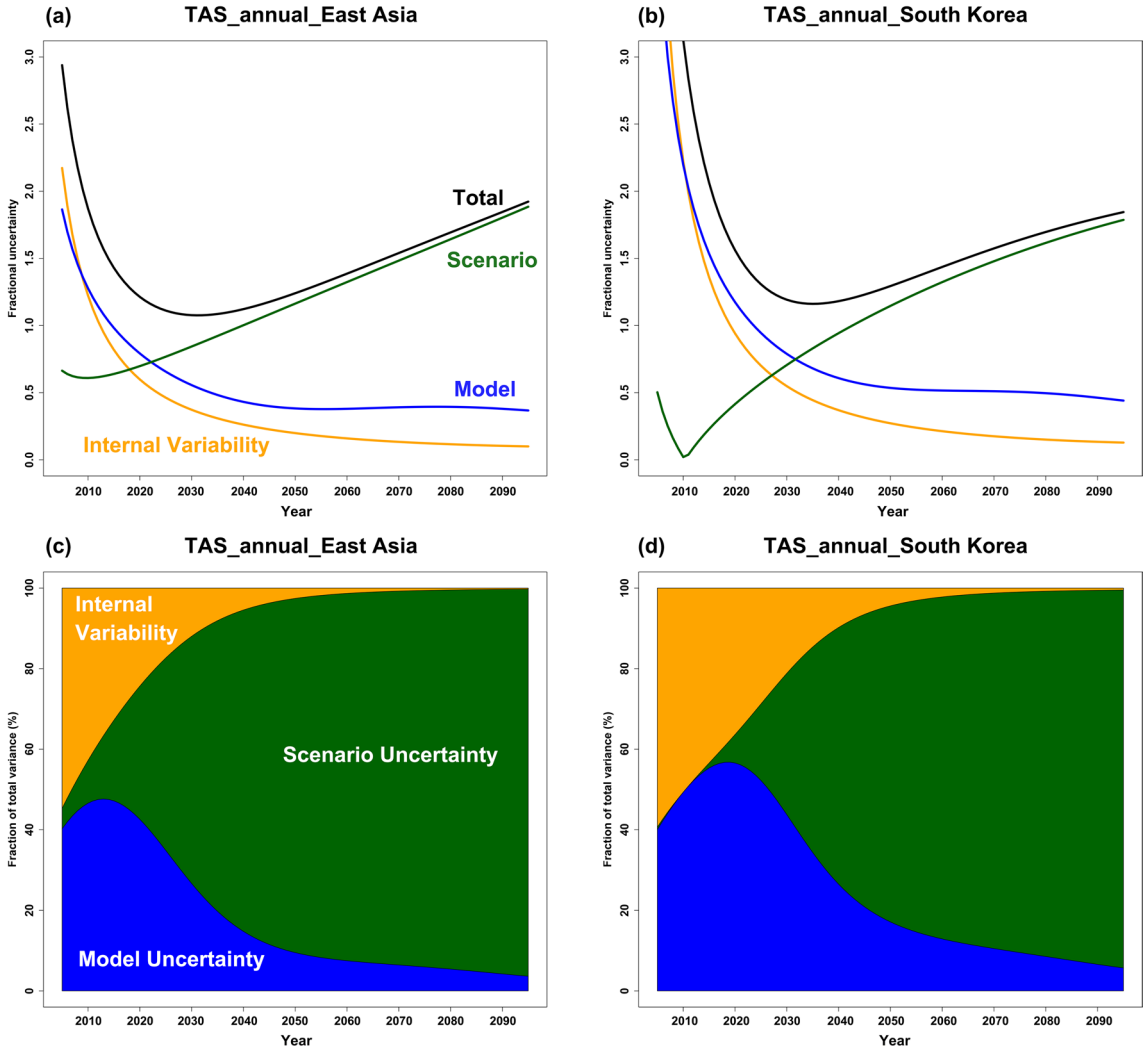

Fig. 3 Temporal changes of **a**, **b** the fractional uncertainties and **c**, **d** the fraction of each component to the total variance for the future projection of the annual means of TAS for bias-corrected RCMs over East Asia and South Korea. The yellow, blue, and green colors indicate the internal variability, model uncertainty, and scenario uncertainty, respectively

other hand, it has been predicted that the internal variability in winter will be very large in the near-term projection.

Similar to TAS, in the case of the East Asian PR, the main uncertainty factors in the annual and all-seasonal means in the near-term projection are the internal variability and model uncertainty (Figs. 5a, c, 6). In the fractional uncertainty, internal variability and model uncertainty tend to decrease as time increases (Figs. 5a, 6a, b). The main difference between the PR and TAS is that the internal variability of the PR considerably contributes to the fraction to the total variance, even in the long-term projections, until approximately the end of the twenty-first century (Figs. 5c, 6c, d). In addition, the inflection point of the total uncertainty does not appear or remains unclear in the fractional uncertainty (Figs. 5a, 6a, b). In the fractional uncertainty for the future projection of the summer mean of PR from Fig. 6a, the total fractional uncertainty during the near-future is predicted to be quite large. According to Eq. 16, total fractional uncertainty is calculated as the ratio of the total variance of the future climate change projections and the mean change of all projections. Thus, the projection for summer PR during the near-future will be smaller than for other PR cases in the same period (Fig. 2), but the total variances for PR will be larger than the annual mean of PR, resulting in Fig. 6a. Over the entire future period, the results obtained for the annual and summer means of PR show that the difference in the physical processes of the RCM is the primary factor affecting the model uncertainty. Therefore, if the physical processes for the PR are improved, the model uncertainties can be decreased, and thus the total uncertainty will also be reduced. On the other hand, in winter with low precipitation, the scenario uncertainty is a considerable contribution factor

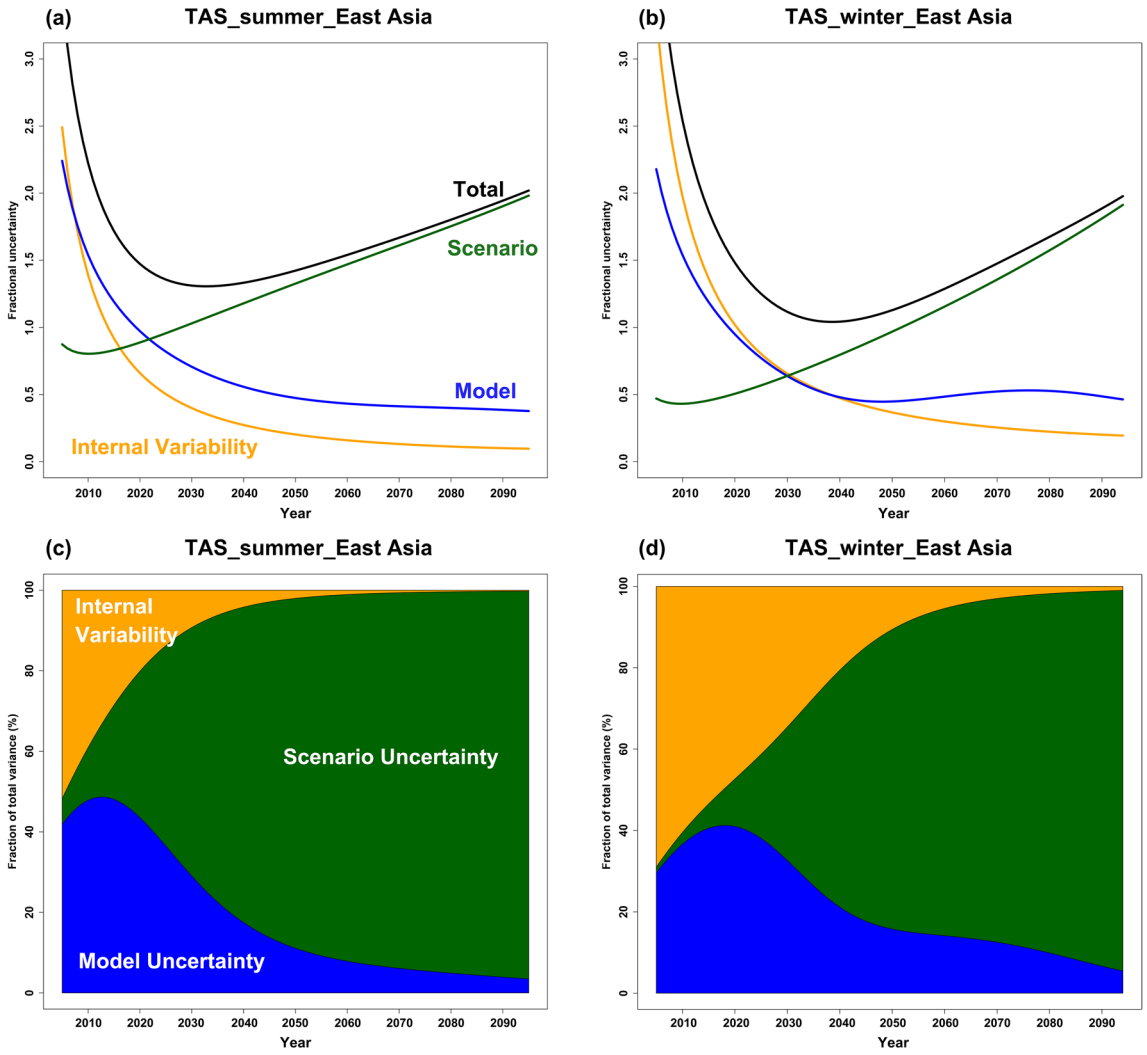

Fig. 4 Temporal changes of **a**, **b** the fractional uncertainties and **c**, **d** the fraction of each component to the total variance for the future projection of the seasonal means of TAS for the bias for bias-corrected RCMs corrected RCMs over East Asia

to the total uncertainty of the long–term projection, so the intensification of climate change signals seems to contribute to this cause (Fig. 6d). In the case of the annual mean of PR over South Korea, the contribution of the internal variability to the total uncertainty is similar to that of the model uncertainty, even in the long-term projection (Figs. 5b, d). Consequently, it can be speculated that the natural variability of the climate system, as well as the physical processes of the model, contribute to the uncertainty of PR over South Korea in the long-term projection. Moreover, as in the case of TAS, the internal variability of PR in South Korea is expected to be larger than that of East Asia in the near-term projection, confirming the importance of the internal variability on the regional or local scales again.

The S/N ratio of the future climate projection, the reciprocal of the total fractional uncertainty, is often used to evaluate the robustness of the prediction. In the case of TAS, the maximum S/N ratio of the annual and winter means was close to 1. However, for both the TAS and PR, it is not expected that the annual and all-seasonal means will exceed 1 in any period (Fig. S1). Furthermore, with respect to the spatial distribution of the S/N ratio, it was predicted that no grids will exceed one in all-seasons and periods of TAS and PR, except for the winter TAS in some parts of northcentral China (Fig. S2). Hawkins and Sutton (2009) reported that, although these results are challenging to assign great value to policy establishment for climate change adaptation, it is a challenge to overcome this through continuous improvement of RCM in the future.

The uncertainty components of future climate projections for East Asia or South Korea have been assessed above. To identify the uncertainty components of future projections at a detailed regional scale over East Asia, the gridded patterns of uncertainty component fractions

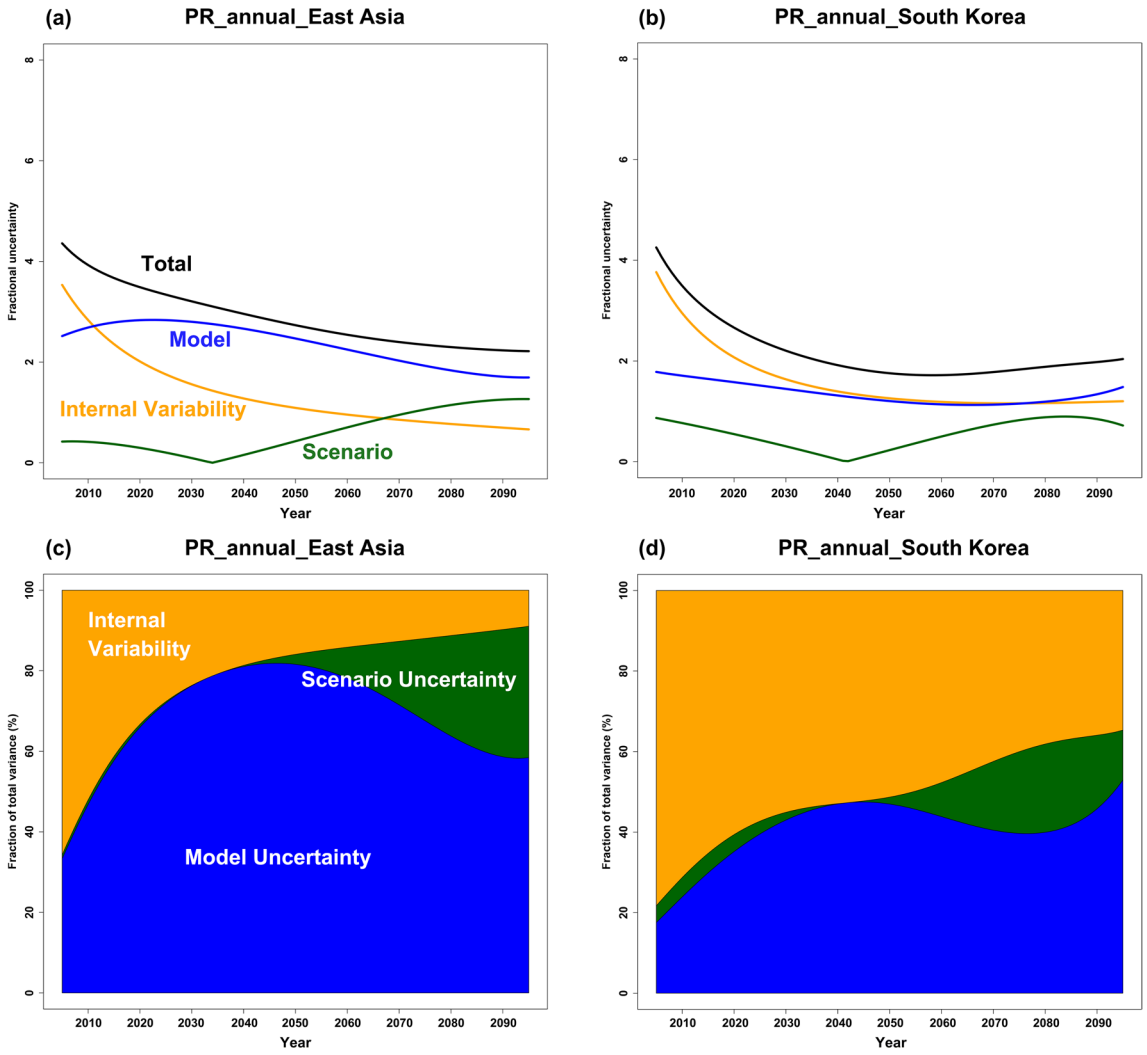

Fig. 5 Same as Fig. 3 but for the annual means of PR

of TAS and PR averaged for the future three periods of decadal means are represented in Fig. 7. Here, if the original spatial resolution of RCM is applied, interpretation at a regional scale is difficult because the difference in the uncertainty component fractions between grids is large (Fig. S3). Therefore, we averaged the future projection values of the grids at a $10° \times 10°$ scale and expressed the uncertainty component fractions of TAS and PR for this. For the annual and all-seasonal means of TAS, it is predicted that, in most grids, the scenario uncertainty will be the dominant component during the 2050s and 2090s. This can also be approximately inferred through the spatial patterns of future TAS projections for the bias–corrected RCMs by scenarios for each model and MME over East Asia for each model and MME (Fig. S4–S6). In most grids, the differences in projections between models are expected to be small under the same scenario for the 2050s and 2090s. In contrast, the MMEs represent that the differences in projections between scenarios for the same time period will be considerably large, which indicates the likelihood of obtaining the aforementioned result. With respect to the fraction of the uncertainty components to the total variance in the 2020s, in the case of the internal variability, the winter mean of TAS will exceed 50% in Hokkaido and eastern Japan. The scenario uncertainties in the 2020s are high in northeastern and central–western China and the Russian *Primorsky Krai* during the summer. This suggests that the anthropogenic warming signals in these regions may intensify earlier than in the other regions. For the annual and all–seasonal means of PR, the internal variability and model uncertainty are predicted to be the dominant components of the uncertainty during all future periods in most grids. The scenario uncertainty will be prominent in northern China and Mongolia during the 2090s for the annual and winter means of PR. Moreover, these results can also be estimated from the prediction that

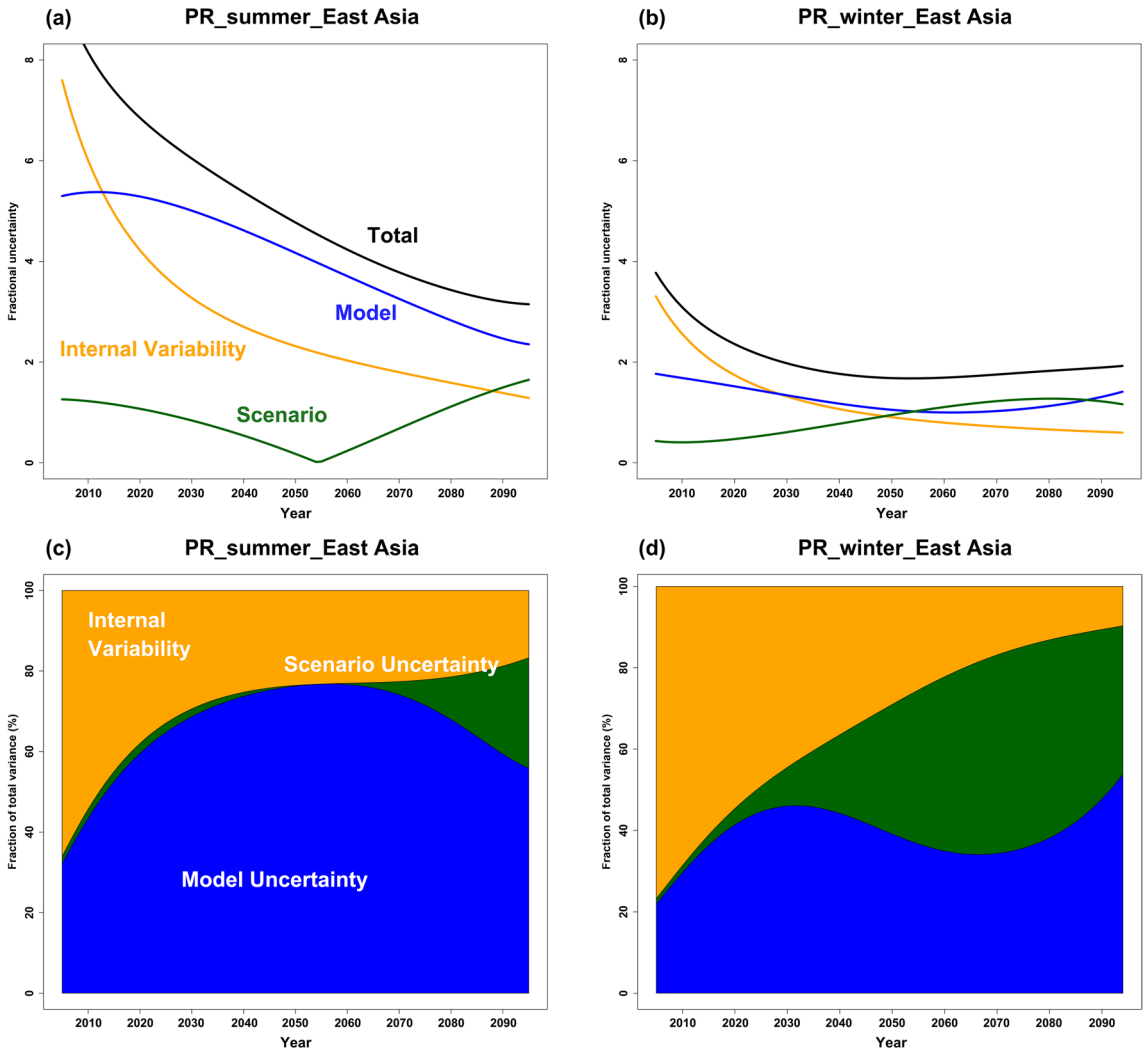

Fig. 6 Same as Fig. 4 but for the seasonal means of PR

the difference in PR projections of the MMEs between the 2090s scenarios in these regions will be larger than in other regions (Fig. S7–S9). Therefore, it is expected that the winter PR mean will make a contribution to the large fraction of scenario uncertainty regarding the future annual mean in this region during the 2090s. Furthermore, future winter PR in this region will likely be sensitive to intensifying anthropogenic warming signals at the end of the twenty-first century. In contrast to the TAS, some regions maintain the contribution of internal variability to the 2090s period in the annual and all–seasonal means. In particular, the internal variability of the winter PR means is predicted to be high in western Japan, northeastern China, and the northern part of the Korean Peninsula. The fraction of the model uncertainty will be > 50% in central and southern China during the 2090s with respect to the annual and seasonal means of PR. This means that the difference in the physical processes of RCMs dominates the uncertainty of PR in this region, even at the end of the twenty-first century.

4 Conclusions and discussions

This study quantitatively evaluated the changes in the uncertainty components of future TAS and PR projections over East Asia using bias-corrected high-resolution multi-RCM datasets. For the TAS, the main uncertainty factors of the annual and all-seasonal means of the near-term projection were the internal variability and model uncertainty, which decrease with time. The scenario uncertainty tended to increase continuously. In summer, the anthropogenic warming signals intensify early in northeastern and central–western China and the Russian *Primorsky Krai*, and thus the scenario uncertainty is predicted to be high from the 2020s. Therefore, in these regions, it appears necessary

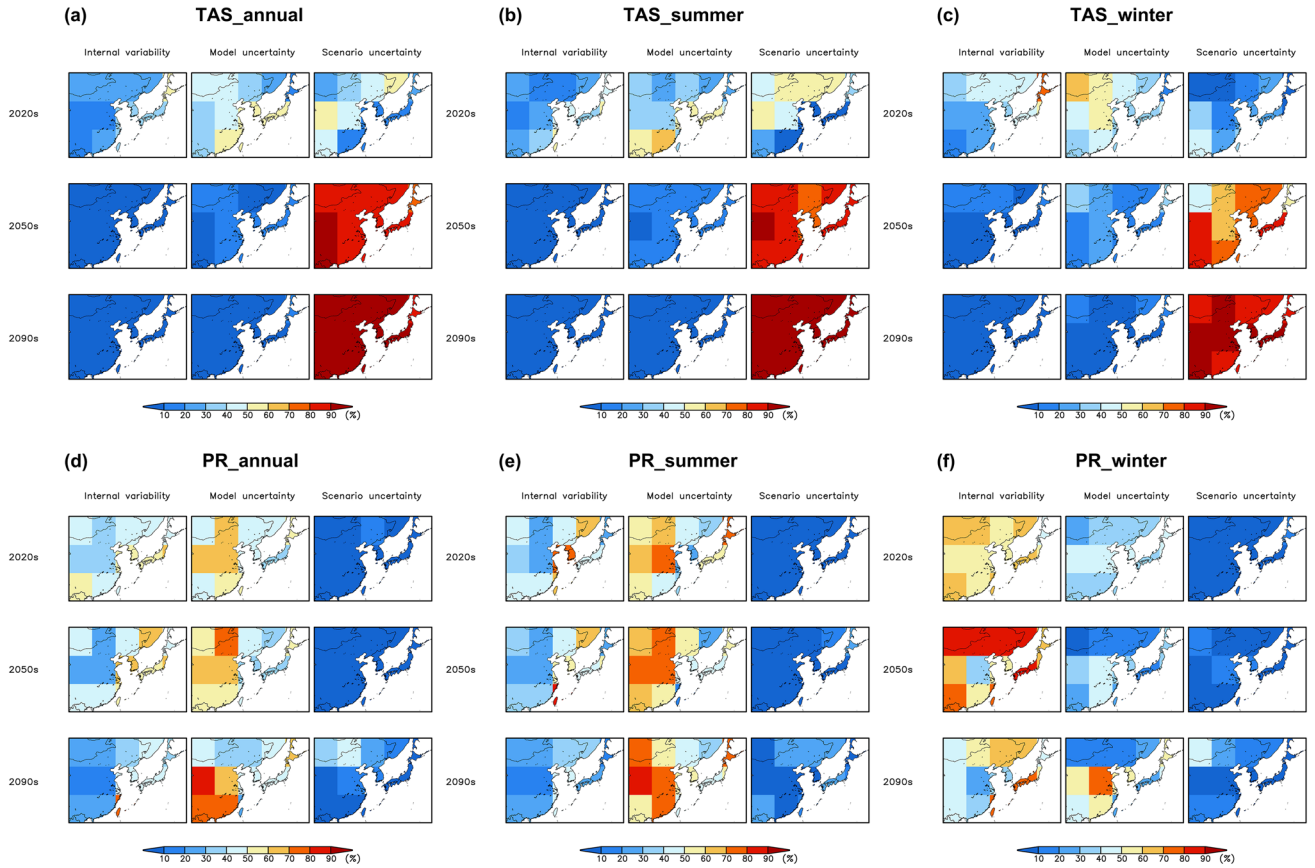

Fig. 7 Gridded patterns of uncertainty component fractions of TAS and PR averaged for the future three periods of decadal means over East Asia at a $10° \times 10°$ grid scale

for decision-makers to promptly establish adaptation plans to prepare for the intensified occurrence of anthropogenic warming signals, which may happen earlier than in other regions.

In the case of PR, the main uncertainty factors affecting the annual average and all-season values of the near-term projection were internal variability and model uncertainty. However, the main difference from TAS was that the PR was predicted to have a considerable internal variability contribution, even in the long-term projection, based on the fraction to the total variance. Based on the results obtained for the annual and summer means of PR, the model uncertainty due to differences in the physical processes among RCMs is a major factor affecting the PR uncertainty. Therefore, as suggested by Zhou et al. (2020), the model uncertainty of PR can be reduced by enhancing the model performance through the improvement of the physical processes, which will eventually decrease the total uncertainty. For both the TAS and PR of the near-term projection, the internal variabilities in the magnitude of the fractional uncertainty and the fraction to the total variance were predicted to be larger in South Korea than those in East Asia.

Concerning the results of the uncertainties estimated for TAS and PR averaged in East Asia, the fraction of the scenario variability to the total uncertainty in the near-term projection was expected to be very small, whereas the contribution of the internal variability was the largest. The internal variability in the near-future can be considerably reduced by enhancing the near-term climate prediction based on progress in climate science, such as advances in observations and an improved scientific understanding (Smith et al. 2007; Hawkins and Sutton 2009, 2011). As a result, the total uncertainty in the near-term projection will also decrease. The total variance (T), obtained by combining the three uncertainty components (Eq. 16), increases over time in both TAS and PR (Fig. S10). Therefore, since uncertainty in the distant future is much larger than in the near future it is difficult to make policy decisions to respond to the projection of climate change in the distant future. As suggested above, since larger uncertainty leads to higher costs for climate change adaptation management (Giorgi 2010), preparing adaptation plans for near-term climate projections with less uncertainty and higher predictive performance is more effective than in

the distant future with larger uncertainty. Thus, because decision-makers establish the long-term climate change adaptation plans based on near-term projections, reducing uncertainties in the near-term prediction is crucial (Cox and Stephenson 2007). To achieve this, it is to reduce internal variability, which has the largest contribution to the uncertainty of the near-term projections. Especially the internal variability is expected to be more prominent in the near-term projection as the spatial scale is smaller, this indicates that reducing internal variability through the improvement of near-term climate prediction at the regional scale is more important than at the continental or sub-continental scale. In particular, at the regional scale, decision-making in near-term planning activities (e.g., agriculture, urban planning, health, etc.) is crucial. Therefore, effective climate adaptation plans for these sectors require the reduction of the near-term uncertainty through the improvement of near-term climate prediction (WCRP 2016; Kushnir et al. 2019). For the TAS, the scenario uncertainty is considerably large in the long-term projection, and the ultimate cause of this is future anthropogenic emissions of greenhouse gases and aerosols. Therefore, reducing the scenario uncertainty depends on human efforts and will for future climate change (Cox and Stephenson 2007). Furthermore, adaptation costs to prepare for the intensification of anthropogenic warming can be reduced by reducing the scenario uncertainty.

This study has a limitation in that the numbers of applied models and future scenarios are relatively small. Nevertheless, it is meaningful as a study in which the components of uncertainty for the future climate projections of East Asia from high-resolution multi-RCMs were assessed in detail for the first time by applying the available data, not GCM, as much as possible. Many studies on future climate projections produce results by the ensembles of several climate models rather than using a single climate model. This is because the results of the MME generally provide more reliable results than when a single climate model is applied (Park et al. 2016; 2020a). As presented in Sect. 1, to obtain reliable future climate projection results by using various climate models, it is required to quantitatively identify uncertainties in climate models and reduce them. The CORDEX-East Asia project team is currently producing high-resolution RCMs for SSP (Shared Socioeconomic Pathways) scenarios, which are being forced by CMIP6 GCMs across the East Asian domain. The results of uncertainty about future climate projections estimated by these the latest RCMs may differ from those of this study. For our upcoming study, we plan to evaluate the uncertainty of future East Asian climate projections by using the RCMs of SSP scenarios produced through the CORDEX-East Asia project and to compare them with the results of the RCP scenarios. Furthermore, we will compare the results according to the difference in the number of scenarios or RCMs applied to the study.

To improve the prediction of climate models, advances in understanding the physics and dynamics of climate are required, and our study will provide sufficient motivation for this. In particular, the role of RCM data produced by dynamically downscaling GCM for effective climate change response on a regional scale is becoming increasingly important in East Asia, which has complicated climate processes as well as a huge population. Therefore, this study can be served as a fruitful reference when improving the simulation performance of RCM developed in the future. Park et al. (2020b) revealed that there would be considerable differences in the fractions of uncertainty components for mean and extreme in future climate projections over Seoul metropolitan city. As mentioned in Sect. 1, East Asia is very vulnerable to climate extremes. Accordingly, it is necessary to identify the difference in the fractions of future uncertainty components between the mean and extreme climates over East Asia, and we plan to conduct this as a follow-up study.

Supplementary Information The online version contains supplementary material available at https://doi.org/10.1007/s00382-023-07006-z.

Author contributions CP: conceptualization, methodology, software, investigation, validation, formal analysis, data curation, and writing—original draft, review, and editing. S-WS and AJ: software, investigation, data curation, and writing—review and editing. D-HC: conceptualization, supervision, funding acquisition, and writing—original draft, review, and editing. S-KM: conceptualization, methodology, data curation, and writing—review and editing. Y-HK: methodology, software, data curation, and writing—review and editing. YC, E-CC, M-SS, J-BA, and Y-HB: data curation and writing—review and editing.

Funding This work was funded by the Korea Meteorological Administration Research and Development Program under Grant KMI(KMI2021-00913).

Data Availability Reanalysis datasets from the Asian Precipitation-Highly Resolved Observational Data Integration Toward Evaluation (APHRODITE) can be accessed from http://aphrodite.st.hirosaki-u.ac.jp/products.html (Yatagai et al. 2012). All bias-corrected RCMs are available at https://doi.org/10.5281/zenodo.7514726 (Park et al. 2023). Figures were made with the R version 3.3.1, available at https://www.r-project.org and the Grads version 2.0.1.oga.1 from http://cola.gmu.edu/grads [Software].

Declarations

Conflict of interest The authors declare that they have no known competing financial interests or personal relationships that could have appeared to influence the work reported in this paper.

References

Ahn JB, Jo S, Suh MS, Cha DH, Lee DK, Hong SY, Min SK, Park SC, Kang HS (2015) Changes of precipitation extremes over South Korea projected by the 5 RCMs under RCP scenarios.

Asia Pac J Atmos Sci 52:223–236. https://doi.org/10.1007/s13143-016-0021-0

Baek HJ et al (2013) Climate change in the 21st century simulated by HadGEM2-AO under representative concentration pathways. Asia Pac J Atmos Sci 49:603–618. https://doi.org/10.1007/s13143-013-0053-7

Booth BBB, Bernie D, McNeall D, Hawkins E, Caesar J, Boulton C, Friedlingstein P, Sexton DMH (2013) Scenario and modelling uncertainty in global mean temperature change derived from emission-driven global climate models. Earth Syst Dyn 4:95–108. https://doi.org/10.5194/esd-4-95-2013

Cha DH, Lee DK (2009) Reduction of systematic errors in regional climate simulations of the summer monsoon over East Asia and the western North Pacific by applying the spectral nudging technique. J Geophys Res Atmos 114:D14108. https://doi.org/10.1029/2008JD011176

Cha DH, Lee DK, Jin CS, Kim G, Choi Y, Suh MS, Ahn JB, Hong SY, Min SK, Park SC, Kang HS (2016) Future changes in summer precipitation in regional climate simulations over the Korean peninsula forced by multi-RCP scenarios of HadGEM2-AO. Asia Pac J Atmos Sci 52:139–149. https://doi.org/10.1007/s13143-016-0015-y

Chen H, Sun J (2015) Changes in climate extreme events in China associated with warming. Int J Climatol 35:2735–2751. https://doi.org/10.1002/joc.4168

Choi YW, Ahn JB, Suh MS, Cha DH, Lee DK, Hong SY, Min SK, Park SC, Kang HS (2016) Future changes in drought characteristics over South Korea using multi regional climate models with the standardized precipitation index. Asia Pac J Atmos Sci 52:209–222. https://doi.org/10.1007/s13143-016-0020-1

Cox P, Stephenson D (2007) A changing climate for prediction. Science 317:207–208. https://doi.org/10.1126/science.1145956

Davies T, Cullen MJP, Malcolm AJ, Mawson MH, Staniforth A, White AA, Wood N (2005) A new dynamical core for the met office's global and regional modeling of the atmosphere. Q J R Meteorol Soc 131:1759–1782. https://doi.org/10.1256/qj.04.101

Evin G, Hingray B, Blanchetm J, Eckert N, Morin S, Verfaillie D (2019) Partitioning uncertainty components of an incomplete ensemble of climate projections using data augmentation. J Clim 32:2423–2440. https://doi.org/10.1175/JCLI-D-18-0606.1

Evin G, Somot S, Hingray B (2021) Balanced estimate and uncertainty assessment of European climate change using the large EURO-CORDEX regional climate model ensemble. Earth Syst Dyn 12:1543–1569. https://doi.org/10.5194/esd-12-1543-2021

Fernández J, Frías MD, Cabos WD et al (2019) Consistency of climate change projections from multiple global and regional model intercomparison projects. Clim Dyn 52:1139–1156. https://doi.org/10.1007/s00382-018-4181-8

Giorgi F (2010) Uncertainties in climate change projections, from the global to the regional scale. EPJ Web Conf 9:115–129. https://doi.org/10.1051/epjconf/201009009

Giorgi F, Mearns LO (1999) Introduction to special section: regional climate modeling revisited. J Geophys Res Atmos 104:6335–6352. https://doi.org/10.1029/98JD02072

Giorgi F, Jones C, Asrar GR (2009) Addressing climate information needs at the regional level: the CORDEX framework. WMO Bull 58:175–183

Giorgi F, Coppola E, Solmon F, Mariotti L, Sylla MB, Bi X, Elguindi N, Diro GT, Nair V, Giuliani G, Turuncoglu UU, Cozzini S, Güttler I, O'Brien TA, Tawfik AB, Shalaby A, Zakey AS, Steiner AL, Stordal F, Sloan LC (2012) RegCM4: model description and preliminary tests over multiple CORDEX domains. Clim Res 52:7–29. https://doi.org/10.3354/cr01018

Guo Y, Cao J, Li H, Wang J, Ding Y (2016) Simulation of the Interface between the Indian summer monsoon and the East Asian summer monsoon: intercomparison between MPI-ESM and ECHAM5/MPI-OM. Adv Atmos Sci 33:294–308. https://doi.org/10.1007/s00376-015-5073-z

Hausfather Z, Peters GP (2020) Emissions—the 'business as usual' story is misleading. Nature 577:618–620. https://doi.org/10.1038/d41586-020-00177-3

Hawkins E, Sutton R (2009) The potential to narrow uncertainty in regional climate predictions. Bull Am Meteorol Soc 90:1095–1107. https://doi.org/10.1175/2009BAMS2607.1

Hawkins E, Sutton R (2011) The potential to narrow uncertainty in projections of regional precipitation change. Clim Dyn 37:407–418. https://doi.org/10.1007/s00382-010-0810-6

Hawkins E, Smith RS, Gregory JM, Stainforth DA (2016) Irreducible uncertainty in near-term climate projections. Clim Dyn 46:3807–3819. https://doi.org/10.1007/s00382-015-2806-8

IPCC (2012) Managing the risks of extreme events and disasters to advance climate change adaptation. In: Field CB et al (eds) A special report of working groups I and II of the intergovernmental panel on climate change. Cambridge University Press, Cambridge

IPCC (2013) Climate change 2013: the physical science basis. In: Stocker TF et al (eds) Contribution of working group I to the fifth assessment report of the Intergovernmental Panel on Climate Change. Cambridge University Press, Cambridge

Kim G, Kim J, Kim CJ, Jin CS, Suh MS, Park SC, Cha DH (2014) Climate change projections over CORDEX East Asia domain using multi-RCMs. J Clim Res 9:257–268. https://doi.org/10.14383/cri.2014.9.4

Kim G, Cha DH, Park C, Lee G, Jin CS, Lee DK, Suh MS, Ahn JB, Min SK, Hong SY, Knag HS (2018) Future changes in extreme precipitation indices over Korea. Int J Climatol 38:e862–e874. https://doi.org/10.1002/joc.5414

Kim G, Cha DH, Park C, Jin CS, Lee DK, Suh MS, Oh SG, Hong SY, Ahn JB, Min SK, Kang HS (2020a) Evaluation and projection of regional climate over East Asia in CORDEX-East Asia phase I experiment. Asia-Pac J Atmos Sci 57:119–134. https://doi.org/10.1007/s13143-020-00180-8

Kim G, Cha DH, Lee G, Park C, Jin CS, Lee DK, Suh MS, Ahn JB, Min SK, Kim J (2020b) Projection of future precipitation change over South Korea by regional climate models and bias correction methods. Theor Appl Climatol 141:1415–1429. https://doi.org/10.1007/s00704-020-03282-5

Knutti R, Allen MR, Friedlingstein P, Gregory JM, Hegerl GC, Meehl GA, Meinshausen M, Murphy JM, Plattner GK, Raper SCB, Stocker TF, Stott PA, Teng H, Wigley TML (2008) A review of uncertainties in global temperature projections over the twenty-First century. J Clim 21:2651–2663. https://doi.org/10.1175/2007JCLI2119.1

Kushnir Y et al (2019) Towards operational predictions of the near–term climate. Nat Clim Change 9:94–101. https://doi.org/10.1038/s41558-018-0359-7

Lee D, Min SK, Jin J, Lee JW, Cha DH, Suh MS, Ahn JB, Hong SY, Kang HS, Joh M (2017) Thermodynamic and dynamic contributions to future changes in summer precipitation over Northeast Asia and Korea: a multi-RCM study. Clim Dyn 49:4121–4139. https://doi.org/10.1007/s00382-017-3566-4

Lee H, Jin CS, Cha DH, Lee M, Lee DK, Suh MS, Hong SY, Kang HS (2019) Future change in tropical cyclone activity over the Western North Pacific in CORDEX-East Asia multi-RCMs forced by HadGEM2-AO. J Clim 32:5053–5067. https://doi.org/10.1175/JCLI-D-18-0575.1

Lehner F, Deser C, Maher N, Marotzke J, Fischer EM, Brunner L, Knutti R, Hawkins E (2020) Partitioning climate projection uncertainty with multiple large ensembles and CMIP5/6. Earth Syst Dyn 11:491–508. https://doi.org/10.5194/esd-11-491-2020

Lopez-Cantu T, Prein AF, Samaras C (2019) Uncertainties in future U.S. extreme precipitation from downscaled climate projections.

Geophys Res Lett 47:e2019GL086797. https://doi.org/10.1029/2019GL086797
Martin GM, Bellouin N, Collins WJ (2011) The HadGEM2 family of Met Office Unified Model climate configurations. Geosci Model Dev 4:723–757. https://doi.org/10.5194/gmd-4-723-2011
Northrop PJ, Chandler RE (2014) Quantifying sources of uncertainty in projections of future climate. J Clim 27:8793–8808. https://doi.org/10.1175/JCLI-D-14-00265.1
Oh SG, Suh MS, Lee YS, Ahn JB, Cha DH, Lee DK, Kang HS (2016) Projections of high resolution climate changes for South Korea using multiple-regional climate models based on four RCP scenarios. Part 2: precipitation. Asia Pac J Atmos Sci 52:171–189. https://doi.org/10.1007/s13143-016-0018-8
Park C, Min SK (2019) Multi-RCM near-term projections of summer climate extremes over East Asia. Clim Dyn 52:4937–4952. https://doi.org/10.1007/s00382-018-4425-7
Park C, Min SK, Lee D, Cha DH, Suh MS, Kang HS, Hong SY, Lee DK, Baek HJ, Boo KO, Kwon WT (2016) Evaluation of multiple regional climate models for summer climate extremes over East Asia. Clim Dyn 46:2469–2486. https://doi.org/10.1007/s00382-015-2713-z
Park C, Cha DH, Kim G, Lee G, Lee DK, Suh MS, Hong SY, Ahn JB, Min SK (2020a) Evaluation of summer precipitation over Far East Asia and South Korea simulated by multiple regional climate models. Int J Climatol 40:2270–2284. https://doi.org/10.1002/joc.6331
Park C, Kim G, Shin SW, Cha DH (2020b) Assessment of the uncertainty for future climate change using bias-corrected high-resolution multi-regional climate models over Seoul Metropolitan City. J Clim Res 15:229–242. https://doi.org/10.14383/cri.2020.15.4.229. (**in Korean with English abstract**)
Park C, Lee G, Kim G, Cha DH (2021) Future changes in precipitation for identified sub-regions in East Asia using bias-corrected multi-RCMs. Int J Climatol 41:1889–1904. https://doi.org/10.1002/joc.6936
Park C, Shin SW, Cha DH, Choi Y, Min SK, Kim YH, Chang EC, Suh MS, Ahn JB, Byun YH (2023) Bias-corrected RCMs. Zenodo. https://doi.org/10.5281/zenodo.7514726
Rockel B, Will A, Hense A (2008) The regional climate model COSMO-CLM(CCLM). Meteorol Z 17:347–348. https://doi.org/10.1127/0941-2948/2008/0309
Skamarock WC, Klemp JB, Dudhia J, Gill DO, Barker DM, Wang W, Powers JG (2005) A description of the advanced research WRF version 2. NCAR Technical note TN-468+STR, 88
Smith DM, Cusack S, Colman AW, Folland CK, Harris GR, Murphy JM (2007) Improved surface temperature prediction for the coming decade from a global climate model. Science 317:796–799. https://doi.org/10.1126/science.1139540
Sperber KR, Annamalai H, Kang IS, Kitoh A, Moise A, Turner A, Wang B, Zhou T (2013) The Asian summer monsoon: an intercomparison of CMIP5 vs. CMIP3 simulations of the late 20th century. Clim Dyn 41:2711–2744. https://doi.org/10.1007/s00382-012-1607-6
Stott PA, Kettleborough JA (2002) Origins and estimates of uncertainty in predictions of twenty-first century temperature rise. Nature 416:723–726. https://doi.org/10.1038/416723a
Suh MS, Oh SG, Lee YS, Ahn JB, Cha DH, Lee DK, Kang HS (2016) Projections of high resolution climate changes for South Korea using multiple-regional climate models based on four RCP scenarios. Part 1: surface air temperature. Asia Pac J Atmos Sci 52:151–169. https://doi.org/10.1007/s13143-016-0017-9
Teutschbein C, Seibert J (2012) Bias correction of regional climate model simulations for hydrological climate-change impact studies: review and evaluation of different methods. J Hydrol 456–457:12–29. https://doi.org/10.1016/j.jhydrol.2012.05.052
van Pelt SC, Beersma JJ, Buishand TA, van den Hurk BJJM, Schellekens J (2014) Uncertainty in the future change of extreme precipitation over the Rhine basin: the role of internal climate variability. Clim Dyn 44:1789–1800. https://doi.org/10.1007/s00382-014-2312-4
von Trentini F, Leduc M, Ludwig R (2019) Assessing natural variability in RCM signals: comparison of a multi model EURO-CORDEX ensemble with a 50-member single model large ensemble. Clim Dyn 53:1963–1979. https://doi.org/10.1007/s00382-019-04755-8
WCRP (2016) Near-term climate prediction. A concept note Submitted to WCRP JSC
Woldemeskel FM, Sharma A, Sivakumar B, Mehrotra R (2016) Quantification of precipitation and temperature uncertainties simulated by CMIP3 and CMIP5 models. J Geophys Res Atmos 121:3–17. https://doi.org/10.1002/2015JD023719
Yatagai A, Kaminguchi K, Arakawa O, Hamada A, Yasutomi N, Kitoh A (2012) APHRODITE: constructing a long-term daily gridded precipitation dataset for Asia based on a dense network of rain gauges. Bull Am Meteorol Soc 93:1401–1415. https://doi.org/10.1175/BAMS-D-11-00122.1
Yip S, Ferro CAT, Stephenson DB (2011) A simple, coherent framework for partitioning uncertainty in climate predictions. J Clim 24:4634–4643. https://doi.org/10.1175/2011JCLI4085.1
Yoon JS, Chung IU, Shin SH (2015) Performance of CMIP5 models for the relationship between variabilities of the North Pacific storm track and East Asian winter monsoon. Atmosphere (korean Meteorological Society) 25:295–308. https://doi.org/10.14191/Atmos.2015.25.2.295. (**in Korean with English abstract**)
Zhou T, Lu LJ, Zhang W, Chen Z (2020) The sources of uncertainty in the projection of global land monsoon precipitation. Geophys Res Lett 47:e2020GL088415. https://doi.org/10.1029/2020GL088415